IEICE TRANSACTIONS

on Communications

DOI:10.23919/transcom.2024EBP3064

This advance publication article will be replaced by the finalized version after proofreading.

A PUBLICATION OF THE COMMUNICATIONS SOCIETY

The Institute of Electronics, Information and Communication Engineers

Kikai-Shinko-Kaikan Bldg., 5-8, Shibakoen 3chome, Minato-ku, TOKYO, 105-0011 JAPAN

PAPER

RSSI-Based Localization Enhancement by Exploiting Interference Signals

Hiroyuki HATANO[†], **Seiya HORIUCHI**[†], **Kosuke SANADA**[†], **Kazuo MORI**[†], **Takaya YAMAZATO**[††], **Shintaro ARAI**[†††], **Masato SAITO**[††††], **Yukihiro TADOKORO**[†††††*], ***and*** **Hiroya TANAKA**[†††††*],

SUMMARY Received Signal Strength Indicator (RSSI)-based localization is of interest in indoor localization systems. In this study, we propose a method to improve localization accuracy using interference-oriented fluctuation. We estimate the distance between target and beacon nodes by utilizing the nodes located around them. When the beacon node transmits a signal to the target for measuring the distance, the surrounding nodes also transmit a copy of the signal. Such signals cause interference patterns at the beacon, thereby randomizing the RSSI. Our developed statistical signal processing enables the estimation of the strength of the received signal with the randomized RSSI. We numerically show that the distance between the target and beacon nodes is estimated with lower error than when using the conventional method. In addition, such accurate distance estimation allows significant improvement in localization performance. Our approach is useful for indoor localization systems, for example, those in medical and industrial applications.

key words: *dither, interference, RSSI, localization, cooperation.*

1. Introduction

Indoor positioning techniques have many applications in a variety of fields [1–4]. For example, in personal care applications, information on the user's position can enhance the capability of smart-home management and healthcare monitoring [5–7]. Additionally, with industrial applications, we can control many facilities based on machines' positions in an efficient manner [8–10]. Generally, determining the distance between nodes based on the signal strength allows us to develop simple positioning devices and methods. In modern wireless communication systems, such as Wi-Fi [11–14], Bluetooth [15–17], RFID [18, 19], and UWB [20–22], electromagnetic signals transmitted within a channel are also used to measure the distance. In recent works, many researchers have attempted to enhance positioning performance, including localization accuracy [23, 24], energy efficiency [15, 25, 26], and latency [27].

Signal strength is usually specified using the Received Signal Strength Indicator (RSSI) at the mobile terminals. However, RSSI includes quantized errors due to analog-to-digital (A/D) conversion, and it does not intrinsically match the amplitude of the received signals, thereby causing incorrect distance estimations. These incorrectly determined distances reduce the accuracy of localization. To overcome this issue, noise-induced linearization has been investigated [28]. This technique is applied in digital signal processing, e.g., in the fields of digital audio and video processing, where it is referred to as dither [29, 30]. Additive noise enables the reconstruction of the signal strength from the stochastic profile, and thus it can reduce the error caused by quantization.

In this study, we propose another approach to dither in RSSI-based localization systems. Instead of additive noise, we explore localization enhancement by exploiting the stochastic behavior of interference-oriented fluctuation. For this purpose, we measure the distance between a target device and a beacon by utilizing surrounding nodes. When the beacon transmits the test signal, herein called the reference signal, to the target device for the RSSI-based distance measurement, the surrounding nodes also transmit a copy of the reference signal. These copies interfere with the reference signal, thereby randomizing the RSSI due to wave propagation. This randomization is similar to adding noise in the dithering approach. By applying statistical processing to the randomized RSSI, we can enhance the accuracy of the estimation of the reference signal strength. Numerical results show that our approach realizes lower error in the distance measurement between the target device and beacon than the conventional method, that is, the case without dither. Moreover, this accuracy enhancement of the distance estimation dramatically improves localization performance.

In conventional dither [30], randomness is induced by additive noise sources. In contrast, our approach creates randomness by utilizing the surrounding nodes. An important point is that the beacon and surrounding nodes transmit the reference signal and its copies with the same communication protocol and at the same time. The target device should observe the sum of all these multiple signals. Thus, the reference signal fluctuates at the target device similarly to the multipath effect in fading channels, because the signals transmitted from the surrounding nodes travel via different paths. This fluctuation plays a role similar to noise in dither, which allows for better accuracy of the distance estimation and subsequently reduces the quantization error via the statistical signal processing. Hence, our approach is different from conventional dither.

[†]The authors are with Mie University, Mie 514-8507, Japan
[††]The authors is with Nagoya University, Furo-cho, Chikusa-ku, Nagoya 464-8603, Japan
[†††]The author is with Okayama University of Science, 1-1 Ridai-cho, Kita-ku, Okayama 700-0005, Japan
[††††]The authors is with University of the Ryukyus, 1, Sembaru, Nishihara-cho, Okinawa 903-0213, Japan
[†††††]The authors are with Toyota Central R&D Laboratories, Inc., Yokomichi, Nagakute, Aichi 480-1192, Japan

The paper is organized as follows. In Section 2, we formulate the problem of RSSI-based distance estimation. Next, we propose a dithering approach with interference-oriented fluctuation and explain the framework of the proposed method. In Section 3, we present a toy model to investigate the basic properties of the proposed method. Also, we numerically analyze the performance limit of the proposed method in comparison with the conventional method in terms of the distance estimation. In Section 4, we discuss localization performance in an indoor environment. Finally, we conclude with some final remarks in Section 5.

2. Problem formulation and proposed method

2.1 Problem formulation

Here, we briefly discuss RSSI-based distance estimation with A/D conversion. We consider a pair of target and beacon nodes and try to measure the distance between them at the target node. When the beacon node transmits a reference signal, the received power of the reference signal in decibels at the target is expressed as [2]

$$p_{\mathrm{r}} = -10a \log d + c, \tag{1}$$

where d is the distance between the target and the beacon, a is the path loss exponent, and c is the received power at a reference distance. The received power can be rewritten as $p_{\mathrm{r}} = 20 \log |v|$ using the signal amplitude $|v|$. Hence, the distance between the target and the beacon is calculated as

$$d = 10^{\frac{c-p_{\mathrm{r}}}{10a}}. \tag{2}$$

Now we consider the RSSI calculator with M-bit resolution and the dynamic range of $p_{\mathrm{high}} - p_{\mathrm{low}}$. Here, p_{high} and p_{low} are the upper and lower limits of the dynamic range, respectively. The received power is quantized with an interval of $\Gamma = (p_{\mathrm{high}} - p_{\mathrm{low}})/2^M$. The power p specified by the RSSI is expressed with a step-wise function $Q(\cdot)$ as

$$\begin{aligned} p &= Q(p_{\mathrm{r}}) \\ &\equiv p_{\mathrm{low}} + \left(m - \frac{1}{2}\right)\Gamma \\ &\quad \text{if } p_{\mathrm{low}} + (m-1)\Gamma \le p_{\mathrm{r}} < p_{\mathrm{low}} + m\Gamma, \end{aligned} \tag{3}$$

where $m = 1, 2, \cdots, M$. The RSSI includes an intrinsic quantization error due to A/D conversion, thereby causing incorrect RSSI-based distance estimations. See the upper panels in Fig. 1. The quantization error, namely the non-zero value of $|p - p_{\mathrm{r}}|$, degrades the accuracy of the distance estimation. A solution to address this issue is presented in the next section. Note that p_{r}, v, and p are functions of time t when the channel fluctuates due to fading and noise. In the equations above, we eliminated the notation (t) to simplify the description.

2.2 Proposed method to improve the distance estimation

A key contribution of this study is the proposal of a method that can overcome the performance degradation coming from the quantization error. In our method, the surrounding nodes transmit the same reference signal as the beacon node, which behaves as an interference signal. The target device should observe the sum of these multiple signals. Thus, the reference signal fluctuates at the target devices similarly to the multipath effect in fading channels, because the signals transmitted from the surrounding nodes travel via different paths. This fluctuation randomizes the RSSI observed at the target node, that is, the interference signals introduce noise. When the statistical behavior (e.g., the slope of probability distribution function (PDF)) of such randomness is known, we can reduce the quantization error via statistical processing, as shown in the lower panels in Fig. 1. This is a

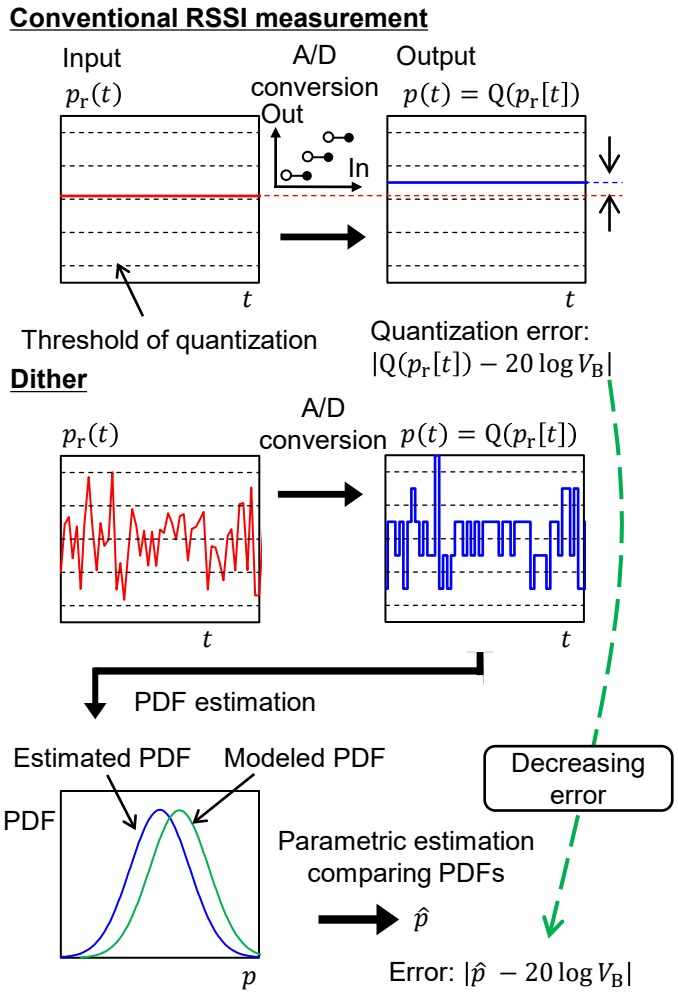

Fig. 1: Approaches for received power estimation based on the conventional RSSI measurement (upper panel) and the proposed dither using interference (lower panel). The received power in the conventional and proposed methods is described as $p_{\mathrm{r}}(t) = 20 \log V_{\mathrm{B}}$ and $p_{\mathrm{r}}(t) = 20 \log |V_{\mathrm{B}} + v_{\mathrm{I}}(t)|$, respectively. Our method calculates the received power with an estimated PDF. We assume a static and noiseless channel, i.e., $v_{\mathrm{B}}(t) = V_{\mathrm{B}} \in \mathbb{R}^+$ and $n(t) = 0$.

kind of noise-aided signal processing method analogous to dither [28–31].

To reveal the contribution of the surrounding nodes, we introduce a propagation toy model where that propagation channel is static and line-of-sight, i.e., there do not exist fading and shadowing effects. Figure 2 shows the system configuration of the proposed distance estimator. A scenario we now consider is the measurement of the distance between the target and beacon nodes surrounded by nodes transmitting the interference signal. The received power at the sampler output is described as

$$\begin{aligned} p[k] &= Q(p_{\mathrm{r}}[k]) \\ &= Q(20\log|v[k]|), \end{aligned} \tag{4a}$$

$$v[k] \equiv v_{\mathrm{B}}[k] + v_{\mathrm{I}}[k] + n[k], \tag{4b}$$

$$v_{\mathrm{I}}[k] \equiv \sum_{l=1}^{L} v_{\mathrm{I},l}[k], \tag{4c}$$

where $p_{\mathrm{r}}[k] = 20\log|v[k]|$, L is the number of the surrounding nodes, $n[k] \in \mathbb{C}$ is noise, and $v_{\mathrm{B}}[k] \in \mathbb{C}$ and $v_{\mathrm{I},l}[k] \in \mathbb{C}$ are respectively the reference and interference signals from the beacon and the l-th surrounding node at the fixed sampling point $k = 1, 2, \cdots, K$. Assuming a static and line-of-sight channel, $v_{\mathrm{B}}[k]$ has a constant value of $V_{\mathrm{B}} \in \mathbb{R}^{+}$.

We should obtain the value of V_{B} to ensure accurate distance estimation. Depending on the node index l, the amplitude and phase of $v_{\mathrm{I},l}[k]$ take different values because each $v_{\mathrm{I},l}[k]$ has a different path length. Generally, a set of received signals, $\{v[1], \cdots, v[K]\}$, is composed of random variables, and accordingly a set of signal powers, $\{p[1], \cdots, p[K]\}$, also consists of random variables. The probability distribution function of $\{p[1], \cdots, p[K]\}$ is expressed as $f(p;\boldsymbol{\theta})$, where $\boldsymbol{\theta}$ denotes the set of parameters of the model including V_{B}. When we know the mathematical model of $f(p;\boldsymbol{\theta})$ but the values of the parameter set $\boldsymbol{\theta}$ are unknown, we can estimate V_{B} using the observed set $\{p[1], \cdots, p[K]\}$.

Note that the PDF given by the RSSI (i.e., the histogram) does not have a smooth shape due to the finite number of data samples. In the PDF estimation based on the finite data sample, the kernel density gives the smooth shape of the estimated function [32]. Kernel density estimation (KDE) is expressed as

$$g(p;\eta) = \frac{1}{K}\sum_{k=1}^{K} G\left(p - p[k];\eta\right), \tag{5}$$

using the Gaussian function as the kernel: $G(p;\eta) = 1/(\sqrt{2\pi}\eta)\exp[-p^2/(2\eta^2)]$, where η^2 is the variance of the kernel. Here, the bandwidth of the kernel is set to unity. To measure the statistical distance between the observed PDF $g(p;\eta)$ and the model $f(p;\boldsymbol{\theta})$, we calculate Kullback-Leibler divergence (KLD), which is described as [33]

$$D = \int_{-\infty}^{\infty} g(p;\eta)\log\left(\frac{g(p;\eta)}{f(p;\boldsymbol{\theta})}\right)\mathrm{d}p. \tag{6}$$

The small value of D means that $g(p;\eta)$ and $f(p;\boldsymbol{\theta})$ have similar slopes.

We can estimate the desired value of the received power, $\hat{p}_{\mathrm{r}} = 20\log\hat{V}_{\mathrm{B}}$, from the following optimization problem:

$$\hat{V}_{\mathrm{B}} = \arg\min_{\boldsymbol{\theta},\eta} D. \tag{7}$$

Hence, we can estimate the distance as

$$\hat{d} = 10^{\frac{c-\hat{p}_{\mathrm{r}}}{10a}}. \tag{8}$$

Note that our method requires controlling the timing and duration of transmission of the reference and its copies, although not strictly. This control can be provided via a coordinator node, as described in Section 4. The coordinator node sends a trigger signal to the beacon and the surrounding nodes to begin transmission of the reference and copy signals. The beacon and surrounding nodes transmit the signal for a sufficiently long period to compensate for delays caused by radio propagation and system latency, enabling the target node to receive the reference and copy signals simultaneously.

3. Performance of the proposed method for distance estimation

3.1 The model

This section describes the evaluation of the performance of the proposed method. In the following discussions, we introduce a simple noiseless model: $n[k] = 0$ for all values of k. We suppose that sets of the real and imaginary parts of $\{v_{\mathrm{I},1}[k], \cdots, v_{\mathrm{I},L}[k]\}$ are Gaussian distributed for any k, i.e., $\mathcal{N}(0,\sigma^2)$, assuming that $|v_{\mathrm{I},l}[k]|$ takes a constant value and $v_{\mathrm{I},l}[k]$ has a random phase for any l and k. Here, $\sigma^2 = E[\sum_l v_{\mathrm{I},l}^2[k]]$ is the variance of the distribution where the operator $E[X]$ denotes the ensemble average of random process X. Then, PDFs of the real and imaginary parts are expressed as $\mathcal{N}(V_{\mathrm{B}}\cos\varphi,\sigma^2)$ and $\mathcal{N}(V_{\mathrm{B}}\sin\varphi,\sigma^2)$, respectively. Note that this assumption is reasonable when the transmission power of the surrounding nodes is well-controlled and the delay spread for $v_{\mathrm{B}}[k]$ and $v_{\mathrm{I}}[k]$ is adequately small.

When we have two independent and normally distributed random variables χ_1 and χ_2, the PDF of $(\chi_1^2 + \chi_2^2)/\sigma^2$ has the noncentral chi-square distribution. The PDF of the received signal in decibels at the target node is expressed as

$$f(p;V_{\mathrm{B}},\sigma) = \frac{10^{\frac{p}{10}-1}\ln 10}{2\sigma^2} e^{-\frac{1}{2\sigma^2}\left(V_{\mathrm{B}}^2+10^{\frac{p}{10}}\right)} I_0\left(\frac{V_{\mathrm{B}}}{\sigma^2}10^{\frac{p}{20}}\right), \tag{9}$$

where I_0 is the modified Bessel function. We address the derivation of (9) in Appendix A. From (9), we obtain $\hat{p}_{\mathrm{r}}$ by optimizing (7) in terms of the parameters $\boldsymbol{\theta} = [V_{\mathrm{B}},\sigma]$ and η, and finally obtain the estimated distance $\hat{d}$ from (8).

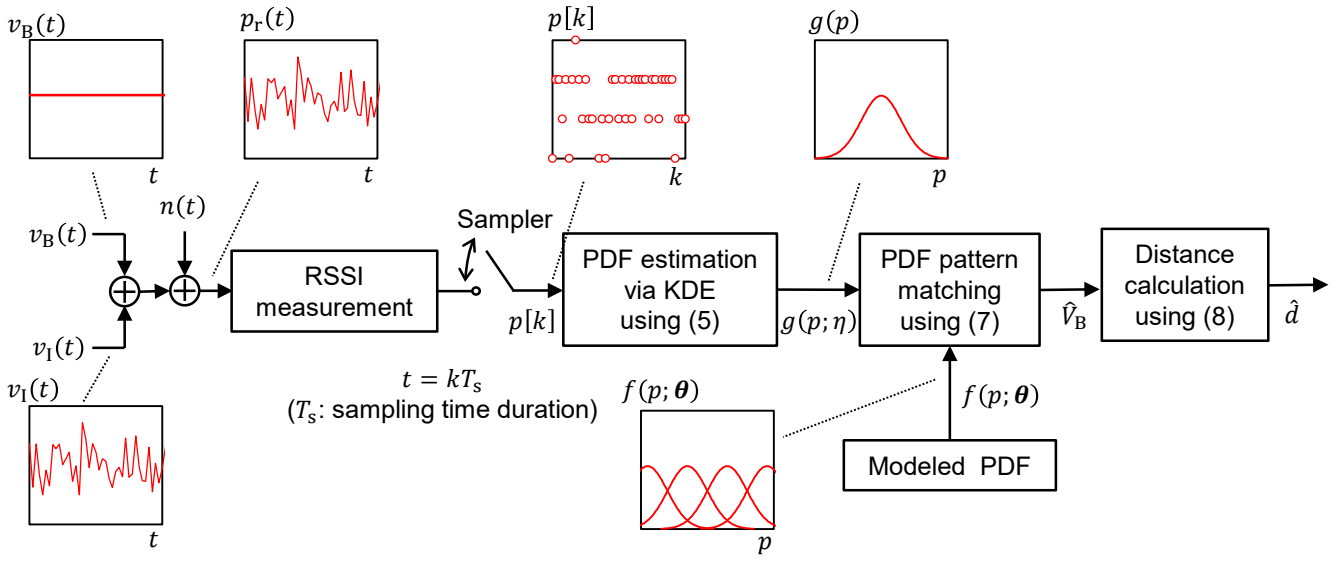

Fig. 2: Schematics of the proposed RSSI-based distance estimator.

3.2 Numerical examples

3.2.1 Performance of distance estimation

Figure 3 shows the error of the distance estimation as the function of the distance between the beacon and target nodes. For the initial setup, we assume that the target and beacon nodes are located at $(x, y, z) = (0, 0, 0)$ and $(x, y, z) = (5, 0, 0)$ in meters, respectively, where $c = -16.0$ and $a = 2$ to give $20 \log V_B = 0$ dBm. The target node is moved along the x axis satisfying $0 \le 20 \log V_B < \Gamma/2$. Then, we had $p[k] = 0$ dBm in the case without dither, so that the estimated distance was $10^{(c-p)/(10a)} = 5$ m in the range of the horizontal axis, as shown in Fig. 3. Thus, the distance error linearly increases with decreasing d in the case without dither, as indicated by the dashed line in Fig. 3. In contrast, the proposed method provides a significant reduction of the estimation error even with large-interval quantization at the RSSI detector (e.g., $\Gamma = 3$ dB). Specifically, the error is lower than 0.4×10^{-4} m for $\Gamma = 1$ dB and 7.1×10^{-4} m for $\Gamma = 3$ dB.

Note that we assumed infinite samples in our simulation; $K \to \infty$ in (5). A detailed treatment is described in Appendix B. Additionally, we used the function "*scipy.optimize.minimize*" in the optimization of (7), which is provided by SciPy 1.6.2.

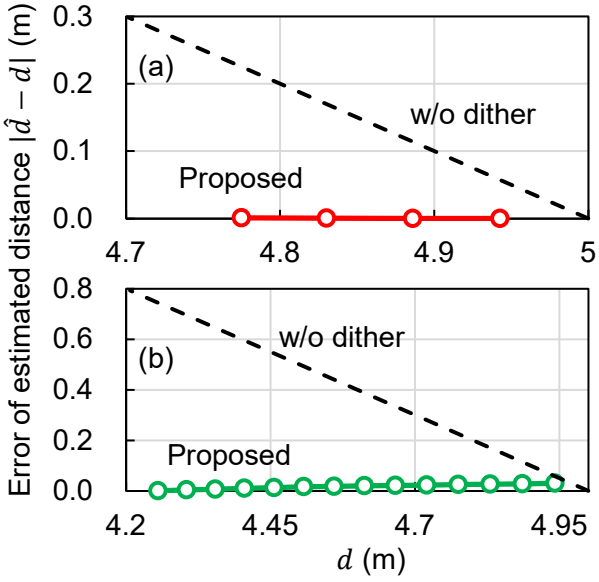

Fig. 3: Absolute value of the distance error, $|\hat{d} - d|$, between the target and beacon nodes for (a) $\Gamma = 1$ dB and (b) 3 dB. The beacon node is located at $(x, y, z) = (0, 0, 0)$. We move the target node from $(x, y, z) = (5, 0, 0)$ in meters toward the negative x direction. Parameters are set as $c = -16.0$ and $a = 2$ to give $20 \log V_B = 0$ dBm at $d = 5$ m. The dashed line is the result obtained with the conventional RSSI-based distance estimator.

3.2.2 Dependency on parameters

We show herein the basic properties of the proposed method. First, we discuss the role of the strength of the interference signals. Figure 4 shows the estimation error as a function of the strength of the interference signals, σ. The smallest value of the estimation error was obtained at $\sigma = 1.5 \times 10^{-2}$ for $\Gamma = 1$ dB and $\sigma = 0.7 \times 10^{-2}$ for $\Gamma = 3$ dB. The optimal result is obtained by fine-tuning the value of σ, and therefore we should control the transmission power of the surrounding nodes to maximize the performance in our dithering approach. This minimization effect in terms of the variance is typical of systems that exhibit stochastic resonance [34]. A similar trend is also found in previous works focusing on the use of interference signals [35, 36].

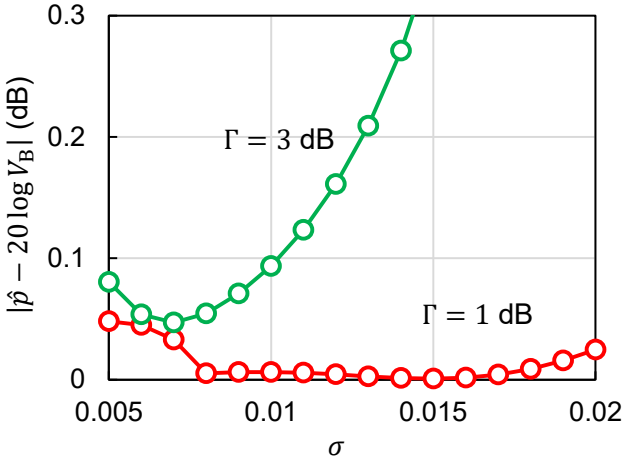

Fig. 4: Error of the received power estimation when $20\log V_B = 0.3$ dBm ($d = 4.83$ m). We assumed an infinite number of samples and optimal η.

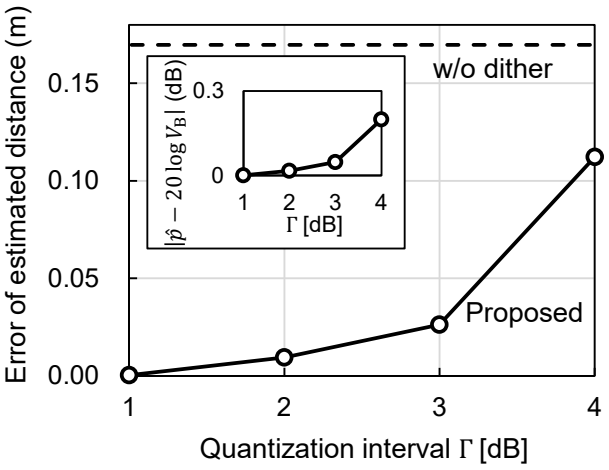

Fig. 5: Lower limit of the estimation error when $20\log V_B = 0.3$ dBm ($d = 4.83$ m). We used optimal σ and η satisfying (7). The dashed line shows the error in the conventional method. The error of the received power estimation is plotted in the inset.

The minimization effect is thus evidence that our analyses are correct.

Second, we point out that the quantization interval Γ is also a key parameter for determining the performance. Figure 5 shows the estimation error as a function of Γ when $20\log V_B = 0.3$ dBm. We used optimal values of σ and η, which give the minimal D according to (7), so that Fig. 5 profiles the lower limit of the estimation error for systems with that specific quantization interval. Interestingly, the proposed method enables greater reduction of the error of the distance estimation in comparison with the conventional method (without dither) even with an interval spacing of the quantization as large as $\Gamma = 4$ dB. The accuracy of the distance estimation is associated with the correctness of the received power estimation, which is plotted in the inset of Fig. 5.

4. Localization enhancement by interference signals

4.1 The model and least squares estimation

We demonstrate the performance of the proposed method for RSSI-based localization. The system includes a mobile node, L surrounding nodes, and a coordinator, as shown in Fig. 6(a). We consider the following scenario. We aim to figure out the position of the mobile node by estimating the distance between the mobile node and surrounding nodes. When the mobile node transmits the reference signal to the l-th surrounding node, the surrounding nodes except for the l-th node transmit the interference signal. At the l-th node, the received power calculated from RSSI is expressed as

$$p_l[k] = Q(20\log|v_l[k]|), \tag{10a}$$
$$v_l[k] \equiv v_{B,l}[k] + v_{S,l}[k]. \tag{10b}$$

Here, $v_{B,l}[k] = V_{B,l} \in \mathbb{R}^+$ is the signal transmitted from the mobile node and $v_{S,l}[k] = \sum_b v_{I,b}[k]$ is the interference signal transmitted from the surrounding nodes except for the l-th node, where $b \in \{a \in \{1,\cdots,L\} | a \neq l\}$. Note that the mobile node and one of the surrounding nodes acts as the *beacon* and the *target* node discussed in Section 3, respectively. The others behave as the surrounding nodes transmitting the interference signal, that is, the surrounding nodes in turn serve as the target node. We emphasize that $p_l[k]$ fluctuates due to the randomness of $v_{S,l}[k]$. Therefore, the proposed estimator shown in Fig. 2 enables more accurate distance estimation than the ordinary RSSI-based distance estimation.

After every surrounding node measures the received power, the dataset of the received power, $\{p_l[1],\cdots,p_l[K]\}$, is collected at the coordinator via wireless communications. The PDF of $p_l[k]$ is described by (9) in Section 3 when we suppose that the real and imaginary parts of $\{v_{S,l}[1],\cdots,v_{S,l}[K]\}$ are Gaussian distributed for any l. From (7) and (8), we can estimate the distance $\hat{d}_l$ between the target node and l-th surrounding node. Using $\{\hat{d}_1,\cdots,\hat{d}_L\}$, the coordinator estimates the position of the mobile node by the least squares approach [37]:

$$\hat{L}_t \equiv [\hat{x},\hat{y},\hat{z}]^T = \left(A^T A\right)^{-1} A^T B, \tag{11a}$$
$$A \equiv \begin{bmatrix} 2(x_1 - x_L) & 2(y_1 - y_L) & 2(z_1 - z_L) \\ \vdots & \vdots & \vdots \\ 2(x_{L-1} - x_L) & 2(y_{L-1} - y_L) & 2(z_{L-1} - z_L) \end{bmatrix}, \tag{11b}$$

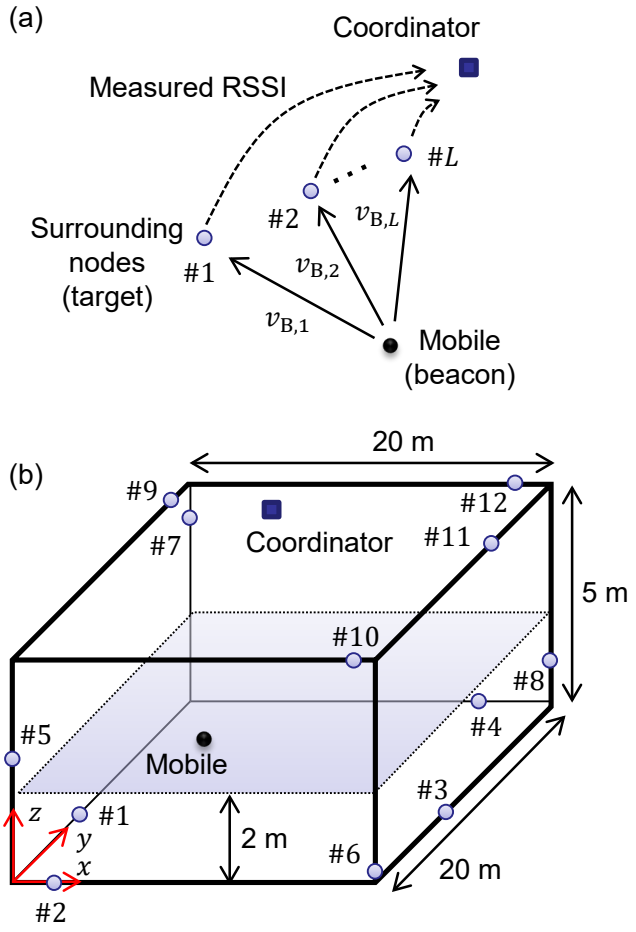

Fig. 6: (a) Node configuration. (b) Node layout. Surrounding nodes (blue-hatched circles) are located at each side of the room. The mobile node is placed on the shaded plane in the region of $2 \le x \le 18$ and $2 \le y \le 18$ in meters, and moves a fixed step of 1 m along the x or y axis at a height of $z = 2$ m.

$$B \equiv \begin{bmatrix} x_1^2 - x_L^2 + y_1^2 - y_L^2 + z_1^2 - z_L^2 + \hat{d}_L^2 - \hat{d}_1^2 \\ \vdots \\ x_{L-1}^2 - x_L^2 + y_{L-1}^2 - y_L^2 + z_{L-1}^2 - z_L^2 + \hat{d}_L^2 - \hat{d}_{L-1}^2 \end{bmatrix}, \tag{11c}$$

where $[x_l, y_l, z_l]^{\mathrm{T}}$ are the coordinates of the l-th surrounding node.

We also tried the conventional RSSI-based method to access the localization performance of the proposed method. In the conventional case, the position was estimated using $d_l = 10^{(c - Q(20 \log V_{\mathrm{B},l}))/(10a)}$ in (11a)-(11c) instead of $\hat{d}_l$.

4.2 Numerical Example

Figure 6(b) shows the layout of the nodes (mobile node, surrounding nodes, and coordinator) in an indoor environment. The size of the room is 20 m × 20 m × 5 m. The coordinator tries to capture the positions of the mobile node located at $L_{\mathrm{t}} = [x, y, z]^{\mathrm{T}}$ in the region of $2 \le x \le 18$ and $2 \le y \le 18$ in meters. The mobile node moves with a fixed step of 1 m along the x or y axis at a height of $z = 2$ m. Table 1 lists the positions of the surrounding nodes, which are randomly allocated at each side of the room. We set $\Gamma = 1$ dB and 2 dB, $\sigma = 0.01$, $a = 2$, and $c = 21.0$.

Table 1: Position of interference nodes

Node index l	x_l (m)	y_l (m)	z_l (m)
1	0	6.6	0
2	2.5	0	0
3	20.0	6.3	0
4	16.9	20.0	0
5	0	0	2.6
6	20.0	0	0.3
7	0	20.0	4.2
8	20.0	20.0	1.5
9	0	18.8	5.0
10	18.2	0	5.0
11	20.0	13.9	5.0
12	18.0	20.0	5.0

Figures 7(a)-(d) show the estimation error, $|\hat{L}_{\mathrm{t}} - L_{\mathrm{t}}| = \sqrt{(\hat{x}-x)^2 + (\hat{y}-y)^2 + (\hat{z}-z)^2}$, for the proposed and conventional localization methods. The proposed method clearly provided a dramatic reduction of the estimation error. In the conventional method, the maps of the estimation error have a specific pattern, e.g., we see diagonal stripes indicated by dashed circles in Fig. 7(d), due to the quantization error of the RSSI measurement. The error of distance estimation periodically increases and decreases depending on the location of the mobile node owing to the quantization. Thus, the distance is correctly estimated in a certain area, but incorrectly in others. In contrast, the proposed method shows a different trend in the maps of estimation error, namely, that the error increases as the mobile moves toward the edge. Specifically, we see relatively large estimation errors at the corners of the room, e.g., $x = 2$ and $y = 2$ in Figs. 7(a) and (c). This comes from the erroneous distance estimation caused by a fixed value of σ. At the corners of the room, the distance between the mobile and the diagonally opposite surrounding node is large, and we have an erroneous distance estimation because of the mismatched σ value. However, as we discussed in Section 3.2.2, there exists an optimal value of σ to obtain the minimum error in the distance estimation. We expect that adaptive control of the transmission power of the surrounding nodes would allow further enhancement of the proposed localization method.

We also plot the cumulative distribution of the estimation error in Fig. 8. We can see that the 90th percentile is 0.05 m ($\Gamma = 1$ dB) and 1.28 m ($\Gamma = 2$ dB) for the proposed method, and 2.76 m ($\Gamma = 1$ dB) and 5.01 m ($\Gamma = 2$ dB) for the conventional method. We conclude that the proposed method enables significant accuracy enhancement in RSSI-based localization systems.

5. Conclusions

We demonstrated a method of RSSI-based localization enhancement utilizing interference signals. The proposed

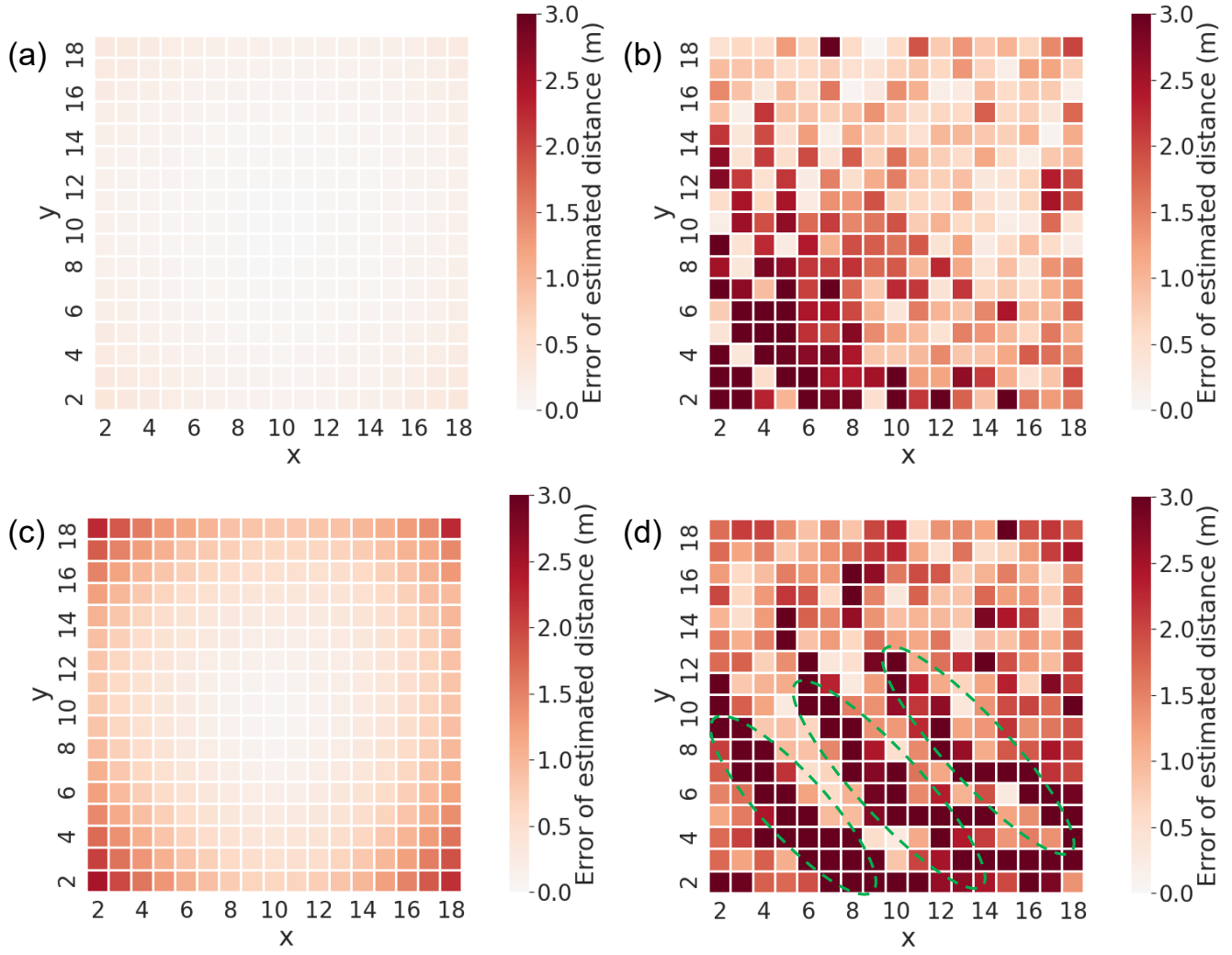

Fig. 7: Maps of estimation error for the proposed method along x and y axes. Grid size of the cell is 1 m. Resolution of the RSSI-detector is Γ =1 dB and 2 dB. (a) Proposed (Γ = 1 dB), (b) conventional (Γ = 1 dB), (c) proposed (Γ = 2 dB), and (d) conventional methods (Γ = 2 dB).

method uses multiple surrounding nodes to transmit copies of a reference signal. The interference signals randomize RSSI and allow for correct distance estimation via a dithering approach. Our numerical analysis shows that such accurate distance estimation provides significant improvement in localization accuracy. In addition, we determined that the strength of the interference signals is the key parameter for maximizing the localization performance.

The proposed method can be considered as a type of fingerprint localization [12–14]. In fingerprint localization, a device takes a local signal reading and compares it to a fingerprint database, then determines its location. The match with the highest similarity to the current reading indicates the device location. In the proposed method, the fingerprint (i.e., the PDF of the RSSI) is associated with the position of the nodes. For accurate localization, our method requires a database of fingerprints of the radio propagation environment. Creating this database is therefore important future work.

Again, the challenge described in this paper is to identify the underlying dithering-mechanism of the proposed method. To reveal the contribution of the surrounding nodes, we introduced a propagation toy model where that propagation channel is static and line-of-sight, i.e., there do not exist fading and shadowing effects. However, the PDF of RSSI is affected by the circumstances in which the systems are used. Specifically, the PDF varies over time when the surrounding environment dynamically change due to the presence of humans, moving objects, etc. It would be fruitful to model the propagation channel including the non-line-of-sight environment with multiple objects and develop a database to implement the proposed localization method in practical systems. More complex models should also be considered, such as the Rician distribution, which is a typical model to describe indoor radio wave propagation. In addition, recent studies have applied machine learning and deep learning techniques

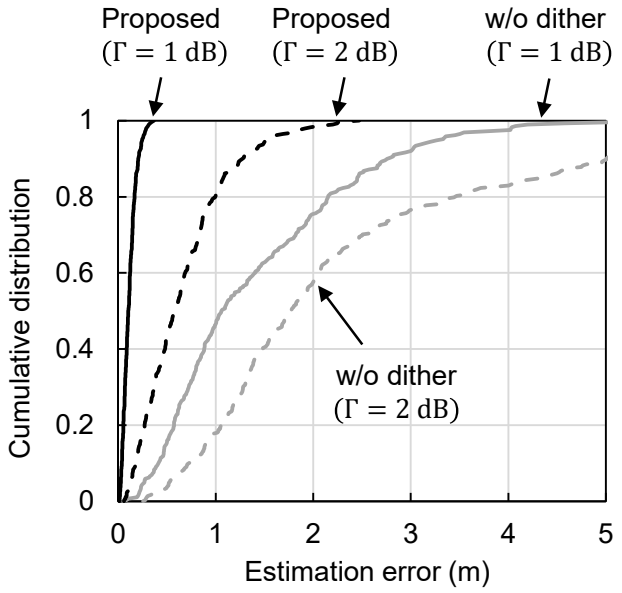

Fig. 8: Cumulative distribution of estimation error.

in fingerprint-based localization. These methods are also candidates for selecting the best fit among the multiple PDFs in our approach. Appropriate database and estimation algorithms would allow the implementation of our method in practical wireless systems.

Appendix A: PDF of the received signal in decibels

We have two independent and normally distributed random variables, $\chi_1 \sim \mathcal{N}(V_\mathrm{B}\cos\varphi, \sigma^2)$ and $\chi_2 \sim \mathcal{N}(V_\mathrm{B}\sin\varphi, \sigma^2)$. The random variable $\chi = (\chi_1^2 + \chi_2^2)/\sigma^2$ is distributed according to the noncentral chi-square distribution α,

$$\alpha(\chi) = \frac{1}{2} e^{-\frac{\chi}{2}-\frac{\lambda}{2}} I_0(\sqrt{\lambda\chi}), \tag{A·1}$$

where $\lambda = V_\mathrm{B}^2/\sigma^2$ is the noncentrality parameter. To measure the received power in the decibel scale, we change the variable χ to $\zeta = 10\log(\sigma^2\chi)$ using the relation $f(\zeta) = \alpha(\chi(\zeta))(\mathrm{d}\chi/\mathrm{d}\zeta)$, and then we have (9).

Appendix B: KDE for infinite samples

When we assume an infinite sample, $K \to \infty$, (5) is rewritten as

$$g(p) = w_m G(p - p_m), \tag{A·2a}$$

$$p_m = p_\mathrm{low} + (m - \frac{1}{2})\Gamma, \tag{A·2b}$$

$$w_m = \int_{p_\mathrm{low}+(m-1)\Gamma}^{p_\mathrm{low}+m\Gamma} f(p)\mathrm{d}p. \tag{A·2c}$$

References

[1] H. Liu, H. Darabi, P. Banerjee, and J. Liu, "Survey of wireless indoor positioning techniques and systems," IEEE Trans. Syst., Man, Cybern. C, vol.37, no.6, pp.1067–1080, 2007.

[2] F. Zafari, A. Gkelias, and K.K. Leung, "A survey of indoor localization systems and technologies," IEEE Commun. Surv. Tutor., vol.21, no.3, pp.2568–2599, 2019.

[3] B. Lashkari, J. Rezazadeh, R. Farahbakhsh, and K. Sandrasegaran, "Crowdsourcing and sensing for indoor localization in IoT: A review," IEEE Sens. J., vol.19, no.7, pp.2408–2434, 2019.

[4] J. Aparicio, F.J. Álvarez, H. Á, and S. Holm, "A survey on acoustic positioning systems for location-based services," IEEE Trans. Instrum. Meas., vol.71, pp.1–36, 2022.

[5] A. Li, E. Bodanese, S. Poslad, T. Hou, K. Wu, and F. Luo, "A trajectory-based gesture recognition in smart homes based on the ultrawideband communication system," IEEE Internet Things J., vol.9, no.22, pp.22861–22873, 2022.

[6] G. Gardašević, M. Veletić, N. Maletić, D. Vasiljević, I. Radusinović, S. Tomović, and M. Radonjić, "The IoT architectural framework, design issues and application domains," Wirel. Pers. Commun., vol.92, no.1, pp.127–148, 2017.

[7] Y.A. Qadri, A. Nauman, Y.B. Zikria, A.V. Vasilakos, and S.W. Kim, "The future of healthcare internet of things: A survey of emerging technologies," IEEE Commun. Surv. Tutor., vol.22, no.2, pp.1121–1167, 2020.

[8] A. Motroni, A. Buffi, and P. Nepa, "A survey on indoor vehicle localization through rfid technology," IEEE Access, vol.9, pp.17921–17942, 2021.

[9] M. Martalò, S. Perri, G. Verdano, F.D. Mola, F. Monica, and G. Ferrari, "Improved UWB TDoA-based positioning using a single hotspot for industrial IoT applications," IEEE Trans. Industr. Inform., vol.18, no.6, pp.3915–3925, 2022.

[10] B.S. Chen, K.C. Yang, and M.Y. Lee, "Robust H∞ nlos-tolerant localization filter and nlos-tolerant remote reference tracking control of mobile robot in wireless sensor networks," IEEE Access, vol.9, pp.164801–164819, 2021.

[11] Z. Zhou, Z. Yang, C. Wu, L. Shangguan, H. Cai, Y. Liu, and L.M. Ni, "WiFi-based indoor line-of-sight identification," IEEE Trans. Wireless Commun., vol.14, no.11, pp.6125–6136, 2015.

[12] J. Jun, L. He, Y. Gu, W. Jiang, G. Kushwaha, V. A, L. Cheng, C. Liu, and T. Zhu, "Low-overhead wifi fingerprinting," IEEE Trans. Mobile Comput., vol.17, no.3, pp.590–603, 2018.

[13] W. Sun, M. Xue, H. Yu, H. Tang, and A. Lin, "Augmentation of fingerprints for indoor wifi localization based on gaussian process regression," IEEE Trans. Veh. Technol., vol.67, no.11, pp.10896–10905, 2018.

[14] P. Chen, J. Shang, and F. Gu, "Learning RSSI feature via ranking model for wi-fi fingerprinting localization," IEEE Trans. Veh. Technol., vol.69, no.2, pp.1695–1705, 2020.

[15] Y. Gu and F. Ren, "Energy-efficient indoor localization of smart hand-held devices using bluetooth," IEEE Access, vol.3, pp.1450–1461, 2015.

[16] J. Zuo, S. Liu, H. Xia, and Y. Qiao, "Multi-phase fingerprint map based on interpolation for indoor localization using ibeacons," IEEE Sensors J., vol.18, no.8, pp.3351–3359, 2018.

[17] T.M.T. Dinh, N.S. Duong, and K. Sandrasegaran, "Smartphone-based indoor positioning using BLE iBeacon and reliable lightweight fingerprint map," IEEE Sensors J., vol.20, no.17, pp.10283–10294, 2020.

[18] F. Martinelli, "A robot localization system combining RSSI and phase shift in UHF-RFID signals," IEEE Trans. Control Syst. Technol., vol.23, no.5, pp.1782–1796, 2015.

[19] H. Chung-Hao, L. Lun-Hui, C.C. Ho, W. Lang-Long, and L. Zu-Hao, "Real-time RFID indoor positioning system based on kalman-filter drift removal and heron-bilateration location estimation," IEEE Trans. Instrum. Meas., vol.64, no.3, pp.728–739, 2015.

[20] B. Yang, J. Li, Z. Shao, and H. Zhang, "Robust UWB indoor localization for NLOS scenes via learning spatial-temporal features," IEEE Sensors J., vol.22, no.8, pp.7990–8000, 2022.

[21] Y. Ibnatta, M. Khaldoun, and M. Sadik, "Indoor localization system based on mobile access point model MAPM using RSS with UWB-OFDM," IEEE Access, vol.10, pp.46043–46056, 2022.
[22] Y. Venkata Lakshmi, P. Singh, M. Abouhawwash, S. Mahajan, A.K. Pandit, and A.B. Ahmed, "Improved Chan algorithm based optimum UWB sensor node localization using hybrid particle swarm optimization," IEEE Access, vol.10, pp.32546–32565, 2022.
[23] K. Wu, J. Xiao, Y. Yi, D. Chen, X. Luo, and L.M. Ni, "CSI-based indoor localization," IEEE Trans. Parallel Distrib. Syst., vol.24, no.7, pp.1300–1309, 2013.
[24] D.D. Nguyen and M. Thuy Le, "Enhanced indoor localization based BLE using gaussian process regression and improved weighted kNN," IEEE Access, vol.9, pp.143795–143806, 2021.
[25] S. Coleri Ergen, H.S. Tetikol, M. Kontik, R. Sevlian, R. Rajagopal, and P. Varaiya, "RSSI-fingerprinting-based mobile phone localization with route constraints," IEEE Trans. Veh. Technol., vol.63, no.1, pp.423–428, 2014.
[26] F. Yaghoubi, A.A. Abbasfar, and B. Maham, "Energy-efficient RSSI-based localization for wireless sensor networks," IEEE Commun. Lett., vol.18, no.6, pp.973–976, 2014.
[27] N. Singh, S. Choe, and R. Punmiya, "Machine learning based indoor localization using Wi-Fi RSSI fingerprints: An overview," IEEE Access, vol.9, pp.127150–127174, 2021.
[28] O. Dabeer and A. Karnik, "Signal parameter estimation using 1-bit dithered quantization," IEEE Trans. Inf. Theory, vol.52, no.12, pp.5389–5405, 2006.
[29] O. Dabeer and E. Masry, "Multivariate signal parameter estimation under dependent noise from 1-bit dithered quantized data," IEEE Trans. Inf. Theory, vol.54, no.4, pp.1637–1654, 2008.
[30] J. Di, A.M. Zoubir, Y. Feng, C. Fritsche, and F. Gustafsson, "Dithering in quantized RSS based localization," 2015 IEEE 6th International Workshop on Computational Advances in Multi-Sensor Adaptive Processing (CAMSAP), pp.245–248.
[31] Y. Nakashima, T. Yamazato, S. Arai, H. Tanaka, and Y. Tadokoro, "Noise-aided demodulation with one-bit comparator for multilevel pulse-amplitude-modulated signals," IEEE Wirel. Commun., vol.7, no.5, pp.848–851, 2018.
[32] B.W. Silverman, Density Estimation for Statistics and Data Analysis, Chapman and Hall, 1986.
[33] S. Kullback and R.A. Leibler, "On information and sufficiency," The Annals of Mathematical Statistics, vol.22, no.1, pp.79–86, 1951.
[34] L. Gammaitoni, P. Hänggi, P. Jung, and F. Marchesoni, "Stochastic resonance," Reviews of Modern Physics, vol.70, no.1, pp.223–287, 1998.
[35] S. Hiraoka, Y. Nakashima, T. Yamazato, S. Arai, Y. Tadokoro, and H. Tanaka, "Interference-aided detection of subthreshold signal using beam control in polarization diversity reception," IEEE Commun. Lett., vol.22, no.9, pp.1926–1929, 2018.
[36] H. Tanaka, S. Hiraoka, S. Arai, T. Yamazato, and Y. Tadokoro, "Direct wireless link to out-of-range node with assistance of surrounding nodes," IEEE Trans. Veh. Technol., vol.68, no.11, pp.10703–10712, 2019.
[37] A. Booranawong, K. Sengchuai, D. Buranapanichkit, N. Jindapetch, and H. Saito, "RSSI-based indoor localization using multi-lateration with zone selection and virtual position-based compensation methods," IEEE Access, vol.9, pp.46223–46239, 2021.

Hiroyuki Hatano received the B.E., M.E. and Dr. Eng. from Nagoya University, Aichi, Japan in 2003, 2005 and 2008, respectively. From 2008 to 2013, he was with Shizuoka University, Shizuoka, Japan. From 2014 to 2019, he was with Utsunomiya University, Tochigi, Japan. Since April 2019, he has been with Mie University, Mie, Japan, where he is currently an associate professor. Also since April 2019, he has been a visiting associate professor at Nagoya University, Aichi, Japan. His current research interests are global navigation satellite system (GNSS), radar/sensor networks, intelligent transport system (ITS) and mobile communication systems. He is a member of IEICE, IPSJ and JSAE. He is also a member of the IEICE ITS research group. He received International Conference on ITST best paper award in 2012, IPSJ ITS research group best paper award in 2014, International Workshop on Informatics best paper award in 2014.

Seiya Horiuchi received his B.E. and M.E. degrees from Mie University in 2019 and 2021 respectively. His research interests are improvement of signal detection performance by using stochastic resonance.

Kosuke Sanada was born in Hokkaido, Japan, on October 20, 1987. He received the B.E. and M.E. Ph.D. degrees from Chiba University, Japan, in 2011, 2012 and 2015, respectively. From October 2015 through February 2016, he was a postdoctoral researcher at the Chiba University. Since March 2016, he has been with Mie University, Mie, Japan, where he is currently working as an Assistant Professor in the division of Electrical and Electronic Engineering, Graduate School of Engineering. His research interests include theoretical analysis, simulation and experiment for IEEE 802.11 in wireless multi-hop networks.

Kazuo Mori received the B.E. degree in computer engineering from Nagoya Institute of Technology, Japan, in 1986 and received the Ph.D. degree in information electronics engineering from Nagoya University, Japan in 2000. In 1986, He joined the Hyper-media Research Center, SANYO Electric Co., Ltd. and was engaged in research and development on telecommunication systems. From 1995 to 2000, he was a research engineer at YRP Mobile Telecommunications Key Technology Research Laboratories Co., Ltd., where he was engaged in research on mobile communication systems. Since August 2000 he has been with Mie University, Japan, where he is currently a Professor in the division of Electrical and Electronic Engineering, Graduate School of Engineering. During 2005–2006, he was a Visiting Research Fellow at King's College London, UK. His research interests include mobile communication systems, wireless sensor networks, radio resource management, and teletraffic evaluation. He received the Excellent Paper Awards from IEICE, Japan in 2002, and from ITE, Japan in 2006.

Takaya Yamazato received the Ph.D. degree from Keio University, Yokohama, Japan, in 1993. He is currently a Professor with the Institute of Liberal Arts and Sciences, Nagoya University, Japan. His research interests include visible light communication, ITS, and e-learning. In 1998, he gave a half-day tutorial entitled "Introduction to CDMA ALOHA" at the IEEE Globecom held in Sydney, Australia. In 2006, he received the IEEE Communication Society's Best Tutorial PaperAward. He served as the Co-Chair of the Wireless Communication Symposia of the IEEE ICC 2009. He was the Co-Chair of Selected Areas in Communication Symposia of the IEEE ICC 2011. From 2008 to 2010, he served as the Chair of the Satellite and Space Communication Technical Committee of the IEEE Communication Society. In 2011, he gave a half-day tutorial entitled "Visible Light Communication" at the IEEE ICC 2011 held in Kyoto, Japan. From 2017 to 2018, he was the Director of Asia/Pacific Board, the IEEE Communication Society. He served as the Editor-in-Chief for the Japanese Section of the IEICE Transactions on Communications from 2009 to 2011.

Shintaro Arai received the B.E., M.E., and D.E. degrees from Tokushima University, Tokushima, Japan, in 2004, 2006 and 2009, respectively. From January 2007 to December 2008, he was a Special Research Student with Nagoya University, Japan. From April 2009 to March 2011, he worked as a Postdoctoral Fellow with the ITS Laboratory, Aichi University of Technology, Japan. From April 2011 to March 2016, he worked as a Research Associate with the National Institute of Technology, Kagawa College, Japan. Since April 2016, he has been a Lecturer with the Okayama University of Science, Japan. His research interests include visible light communication systems, chaos-based communication systems, and stochastic resonance phenomena. He is a Member of the IEICE.

Masato Saito received the B.E., M.E., degrees and Ph.D. degree in engineering from Nagoya University, Aichi, Japan, in 1996, 1998, and 2001, respectively, all in Information Electronics Engineering. He was an Assistant Professor with Nara Institute of Science and Technology (NAIST), Nara, Japan, from 2001 to 2010. Since 2010, he has been an Associate Professor with University of the Ryukyus, Okinawa, Japan. From April 2007 to March 2008, he was a Visiting Researcher at ARC Special Research Centre for Ultra-Broadband Information Networks (CUBIN), the University of Melbourne, Melbourne, Australia. He is a member of IEICE. His research interests include antenna pattern multiplexing for receive diversity, stochastic resonance for wireless communications, modulation schemes for mobiel and satellite communications.

Yukihiro Tadokoro received the B.E., M.E., and Ph.D. degrees in information electronics engineering from Nagoya University, Aichi, Japan, in 2000, 2002, and 2005, respectively. Since 2006, he has been with the Toyota Central Research and Development Laboratories., Inc. He was a Research Scholar with the Department of Physics and Astronomy, Michigan State University, East Lansing, MI, USA, in 2011 and 2012, to study nonlinear phenomena for future applications in signal and information processing fields. Since 2019, he has been a Visiting Professor with the Graduate School of Informatics, Nagoya University. His current research interests include nanoscale wireless communication, noise-related phenomena in nonlinear systems, and their applications in vehicles and nanoscale systems. Dr. Tadokoro is a Senior Member of the Institute of Electronic, Information and Communication Engineers, Japan.

Hiroya Tanaka received the B.E. degree from Saitama University, Saitama, Japan, in 2003, and the M.E. and D.E. degrees from the Tokyo Institute of Technology, Tokyo, Japan, in 2005 and 2008, respectively. Since 2008, he has been with the Toyota Central Research and Development Laboratories Inc. His current research interests are micro/nano-structured electromagnetic devices, nonlinear signal processing, and applied radio instrumentation and measurements. He is a member of the Japan Society of Applied Physics.